International Journal of Renewable Energy Resources 13 (2023) 32-48
https://doi.org/10.22452/ijrer.vol13no2.1

CARBON MONOXIDE-RESISTANT ANODE CATALYSTS FOR SINGLE-CELL DIRECT CARBON MONOXIDE FUEL CELLS: PLATINUM-RUTHENIUM ANODE ELECTROCATALYSTS

Farshid Zabihian[1,*], Asad Davari[2] & Gifty Osei-Prempeh[3]
[1]Department of Mechanical Engineering, California State University Sacramento, Sacramento, CA, U.S.A.
[2]Electrical & Computer Engineering Department, West Virginia University Institute of Technology, Beckley, WV, U.S.A.
[3]Chemical Engineering Department, West Virginia University Institute of Technology, Beckley, WV, U.S.A.
*e-mail: farshid.zabihian@csus.edu

Abstract

The objective of this paper is to present the results of experimentations on the state-of-the-art anode electrocatalysts and the membrane-electrode assemblies (MEAs) developed for direct carbon monoxide fuel cells (DCMFCs). The custom-made platinum-ruthenium (Pt-Ru) MEAs along with a commercial MEA were tested to evaluate the impacts of cell temperature, different types of fuel and oxidant, the flow rate of fuel and oxidant, and humidification temperature on the performance of the MEAs. It was shown that both the catalyst manufacturing process and the test procedure are repeatable. Also, it was shown that the performance of Pt-Ru cells when fueled by CO and CO-containing fuels was markedly inferior to that of hydrogen-fueled fuel cells. However, there were some promising signs that with the right catalysts and optimum operating conditions, the performance of DCMFCs can be significantly improved. It was also shown that increasing the operating temperature always improved the performance. While increasing the flow rates of the reactants improved the performance of the MEAs, there was a limit to this improvement. Furthermore, generally speaking, the performance of the MEAs was better when fed with CO rather than CO-N_2 and O_2 rather than air but the actual impact depended on other operating conditions.

Keywords: Fuel Cell; Carbon Monoxide; Catalysts; Platinum-Ruthenium (Pt-Ru); Coal

1. INTRODUCTION

Coal as a source of energy for electricity generation is still playing a major role in many parts of the world. The United States Department of Energy (DOE) has been promoting "clean coal" technologies as one of the paths to sustainable power generation (Clean Coal Research, 2023). Fuel cell technologies can be an important component of this path. The most obvious and presumably straightforward approach for the utilization of carbon in general and coal in particular as a fuel for a fuel cell is directly feeding them to the fuel cell. This type of fuel cell is called a direct carbon fuel cell (DCFC). They are devices where solid carbon from various sources, such as coal; petroleum coke; woods, grass, and other biomass; and organic garbage, is converted to electricity with no intermediate combustion or gasification. These fuel cells have several characteristics that other types of fuel cells, in that matter any other power generation systems, find almost impossible to compete with, at least theoretically. The thermodynamic electrochemical efficiency of this type of fuel cell is very high (Ozalp et al., 2022). For a process involving an electrochemical reaction, thermodynamic efficiency is defined as the ratio of the change in the Gibbs energy to the change in the enthalpy. For the electrochemical reaction of carbon, the change in the Gibbs energy (394,360 kJ/kmol) is slightly greater than the change in the enthalpy (393,520 kJ/kmol) which results in slightly higher than 100% thermodynamic efficiency. Also, since the fuel and the product are in different phases (solid carbon and gaseous carbon dioxide, respectively), the fuel utilization factor of the fuel cell can theoretically be 100%. This can lead to an actual electrical efficiency of about 90% for DCFCs compared to about 60% and 45% for methane and hydrogen-fueled fuel cells, respectively (Ozalp et al., 2022; Cao et al., 2007). The operating temperatures of DCFCs are high, typically higher than 500°C. The most common electrolytes for DCFCs are molten carbonate, molten hydroxide, and oxygen ion conducting ceramic (Wang et al., 2020a). Power densities up to 124, 140, and 50 mW/cm^2 have been reported for each of these electrolytes, respectively (Cao et al., 2007). In some designs, the anode is made of carbon and is consumed as the fuel while in others the carbon particles (e.g. carbon black or pulverized carbon) suspended in a liquid or air are used as the fuel. DCFCs are in their early stages of development and are facing many challenges. They typically use the components developed for molten carbonate fuel cells (MCFC) and solid oxide fuel cells (SOFC). The impact of coal impurities, the ash effects, the extent of fuel pretreatment, thermal management, and many other details remain to be figured out (Jiang et al., 2017). Overall, the practical use of solid coal or carbon electrochemistry for power generation in DCFCs is quite an engineering challenge. Besides the technological immaturity of DCFCs, their high operating temperatures make them unsuitable for portable applications. A practical approach to address the problem with solid fuels is to preprocess carbon/coal and convert the solid fuel to gaseous or liquid fuels.

Solid fuels can be gasified and converted to gaseous fuels through the gasification process. Alternatively, solid fuels can be converted to liquid fuels, such as methanol, formic acid, or glycerol. The manufacturing process to convert carbon/coal to liquid fuels is complex and energy-intensive; thus, unsuitable for portable applications.

Currently, two carbon/coal preprocessing technologies are commercially available to gasify carbon/coal: gasification and partial oxidation (POX). In the gasification process, carbon reacts with oxygen and steam to generate syngas consisting of carbon monoxide, hydrogen, methane, carbon dioxide, and water vapor.

$2C + O_2 \rightarrow 2CO$

$C + H_2O \rightarrow H_2 + CO$

To increase the concentration of hydrogen, syngas may undergo the following water gas-shift reaction:

$CO + H_2O \rightarrow CO_2 + H_2$

The gasification process is technologically mature and available; however, it requires a lot of water. This high water demand may not be a significant problem for stationary industrial applications but is a major problem for portable applications. The partial oxidation process is the combustion of carbon with insufficient air needed for complete combustion (sub-stoichiometric combustion).

$2C + O_2 \rightarrow 2CO$

In this process, about 30% of the thermal energy content of the fuel is lost during the process (The Gibbs free energy change, ΔG, of carbon oxidation is -394 kJ/mol compared to -283 kJ/mol for carbon monoxide oxidation). However, the CO oxidation is still more energetic than that of hydrogen (ΔG of -283 kJ/mol for CO vs. -237 kJ/mol for H_2), which means the volumetric energy density of carbon monoxide is higher than that of hydrogen. Considering the simplicity of the partial oxidation process and the fact that no water is required for the carbon/coal preprocessing, carbon monoxide is the most convenient carbon/coal-based fuel for portable applications.

With the conversion of the solid fuel to the gaseous fuel, a new avenue for utilization of available fuel cell technologies becomes accessible because a lot of existing fuel cell hardware designs can be adapted for carbon-based fuel cells. The low operating temperature, high current density, simple design, and high-power density (volume-based) among other characteristics make proton exchange membrane fuel cells (PEMFCs), an ideal candidate for portable applications. They typically operate at low temperatures (less than 100°C) although high-temperature PEMFCs (between 100°C and 200°C) are also being developed (Haider, et al., 2021).

The operation of the carbon monoxide PEMFC is simple but the main challenge is the difficulty of the low-temperature electrooxidation of carbon monoxide. The most common electrocatalysts used in the anode electrode of PEMFCs are platinum-based catalysts. These catalysts are poisoned in the presence of CO because of the strong adsorption of CO and the high potential required for CO stripping (around 0.8V vs. NHE). At low temperatures, the surface of the catalyst is covered by CO as a result of the high affinity of carbon monoxide molecules to platinum molecules at the surface of the catalyst (Bıyıkoğlu, 2005). The effect was first documented for PEMFCs by Gottesfeld and Pafford (1998). They illustrated that this problem can be present even with a low concentration of CO. The answer to this problem is to develop anode electrocatalysts with high CO tolerance. The source of inspiration in this regard may come from direct alcohol fuel cells (DAFCs).

The best fuel for the optimum performance of PEMFCs is hydrogen which can be directly provided through a storage system or can be produced in a reformer using liquid fuels. However, the lack of infrastructure for the former and the high cost and weight of the latter prevent their widespread commercialization. To overcome the fuel problem, a great deal of research has been dedicated to the direct utilization of different alcohols in PEMFCs. In direct alcohol fuel cells, methanol (in direct methanol fuel cells, DMFC) or ethanol (in direct ethanol fuel cells, DEFC) is directly fed to a PEMFC as the fuel. Similarly, direct formic acid fuel cells (DFAFC) are fueled by formic acid. These fuel cells are particularly suitable for electric vehicles and portable electronic devices due to their simple construction, relatively high efficiency, and compactness (Alias, et al., 2020; Xia et al., 2019).

The utilization of ethanol (C_2H_6O) as the fuel instead of methanol (CH_3OH) is preferable because of the nontoxic nature, low volatility, higher energy content, low cost, and easy transportation of ethanol as well as the fact that it can be produced from renewable energy sources. However, DEFC faces some challenges, including the difficulty of the complete oxidation of ethanol to CO_2 and the difficulty in breaking C – C bonds using electrocatalysts at low temperatures (unlike methanol which does not have such a bond).

The following three electrochemical reactions are for the anode, cathode, and overall reactions in DMFCs:

Anode: $CH_3OH + H_2O \rightarrow CO_2 + 6H^+ + 6e^-$

Cathode: ${}^3\!/_2\, O_2 + 6H^+ + 6e^- \rightarrow 3H_2O$

Overall: $CH_3OH + {}^3\!/_2\, O_2 \rightarrow CO_2 + 2H_2O$

These electrochemical oxidation reactions need electrocatalysts. It has been established that the most electrochemically active catalyst for these small organic molecules is platinum (Zuo et al., 2022; Xia et al., 2019; Xu et al., 2006). However, in practice, during the electrooxidation of these molecules at low temperatures, carbon monoxide is generated. This intermediate byproduct can poison the platinum electrocatalyst because of the strong carbon monoxide adsorption on the catalyst surface.

Hamnett (1997) provided a twelve-step sequence of reactions for the methanol electrochemical reaction. One of these steps is the adsorption of carbon monoxide on the surface of the Pt catalyst. The oxidation of these adsorbed carbon monoxide species is slow and the rate-determining step (Zuo et al., 2022; Steele & Heinzel, 2001). DEFCs are facing similar problems at an even higher magnitude (Zheng et al., 2020; Lamy et al., 2004), similar to DFAFCs (Ramli et al., 2023). Besides this problem, the high cost of platinum and the loss of catalytic activity are also major problems for Pt catalysts. The problem that the CO-fueled fuel cell is facing, in nature, is similar to the problem that the above-mentioned fuel cells are facing. It is, therefore, reasonable to consider DMFCs, DEFCs, and DFAFCs as the source of inspiration for developing anode electrocatalysts for direct carbon monoxide fuel cells (DCMFCs) and validation of the experimental results. This is particularly important because there are very few papers in the literature on electrocatalysts for DCMFCs, especially for low-temperature operations. Most data in the literature on anode electrocatalysts with improved carbon monoxide tolerance/activity are for DMFCs and to a lesser extent for DEFCs and DFAFCs.

As noted previously, in the presence of carbon monoxide, the surface of platinum is poisoned by strongly adsorbed CO, which almost completely covers the catalyst surface at low potentials (less than 0.5-0.6 V). To reduce or eliminate the problem, Gottesfeld and Pafford (1988) proposed adding a small amount of oxygen or air flow to the anode to oxidize CO to CO_2. Others have proposed CO removal from the fuel flow by the selective catalytic oxidation process (Neri et al., 2014). However, the direct injection of oxygen into the fuel flow in the anode is not practical due to safety concerns (Schmidt et al., 1997a). Schmidt et al. (1997a) proposed adding hydrogen peroxide, H_2O_2 (stored in a separate tank), to the humidifier. Each molecule of H_2O_2 is dissolved to produce H_2O and ½ O_2. These approaches are not appropriate for addressing the problem in this case.

A more practical approach is to add specific metals to platinum (Pt) that are capable of activating water at low potentials to generate oxygenated species, such as adsorbed OH, which in turn can oxidize CO and prevent Pt poisoning. There is a limited number of metals with this characteristic that has long-term stability in an acidic environment (Lamy et al., 2004). It is well established that platinum alloyed with some transition metals, such as ruthenium, can remarkably improve both the electrochemical activity of Pt-based catalysts and their carbon monoxide poisoning resistance (Xu et al., 2006). Platinum-ruthenium electrocatalysts are commonly used for this purpose. A third and even fourth metal have also been added to further improve the performance of anode electrocatalysts.

The originality of this paper can be expressed in two ways. First, the idea of using CO as fuel for PEMFCs is novel and has not been previously explored in the literature. Second, while many papers have been dedicated to the development and study of a wide variety of electrocatalysts that could tolerate different concentrations of CO in fuel for DMFCs, DEFCs, and DFAFCs, the manufacturing process and test conditions were different in each study. This inconsistency makes the comparison of the results of these studies and the identification of the optimum catalyst difficult, if not impossible. In this study, many catalysts were developed using the same process and were tested at comparable conditions, which makes the comparison of their performance and the identification of the best catalysts possible.

The objective of this paper is to present the results of tests on the low to medium-temperature state-of-the-art anode electrocatalysts and the membrane-electrode assemblies (MEAs) developed for carbon monoxide-fueled proton exchange membrane fuel cells (PEMFCs).

In the rest of this paper, some of the most promising electrocatalysts selected based on the information available in the literature are developed and tested at various operating conditions using carbon monoxide, the mixture of CO and N_2, and H_2 as the fuels starting with Pt/Ru, both commercial and homemade, in this paper, followed by other binary, ternary, and quaternary alloys of platinum in the companion paper (Zabihian et al., 2023).

2. METHODOLOGY

The ultimate objective of this project was to develop the complete package for a direct carbon monoxide fuel cell (DCMFC) electricity generation unit for portable applications. This included the development of the gasifier and the fuel cell. In this paper and the following one (Zabihian et al., 2023), the first step which is the design and fabrication of appropriate MEAs are presented along with the results of experimentations conducted on them. Fig. 1 illustrates the simplified flow diagram of the proposed portable electricity generation unit. In this design, carbon or coal is first fed to the dry POX gasifier where it is converted to the gas mainly composed of carbon monoxide (CO) in the presence of oxygen. Then, the hot CO-rich flow is cooled down in a heat exchanger. The flow then enters the anode of the PEM fuel cell as the fuel along with the flow of air or oxygen to the cathode as the oxidant. Within the fuel cell, the electrochemical oxidation of CO generates electricity.

In the proposed carbon monoxide-fueled PEMFC, CO is fed to the anode electrode as the fuel. In the presence of water, carbon monoxide is electrooxidized to carbon dioxide, protons (H^+), and electrons. The flow of electrons produces the desired product, electricity. The protons traverse through the membrane to the cathode. In the cathode, along with the electrons, they react with oxygen to produce water. This water in the cathode outlet can be captured and recycled to the anode. The half-reactions and the overall reactions are as follows:

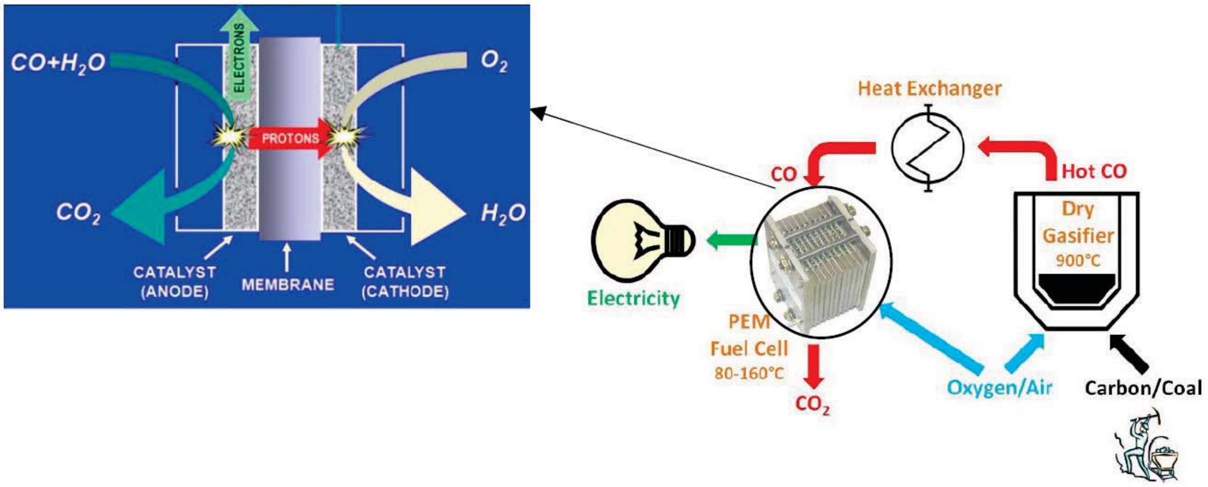

Fig. 1. Simplified flow diagram of the carbon/coal-fueled electricity generation unit including the direct carbon monoxide fuel cell (DCMFC) and the gasifier.

Anode: $\mathrm{CO + H_2O \rightarrow CO_2 + 2H^+ + 2e^-}$

Cathode: $\mathrm{{}^1\!/_2\, O_2 + 2H^+ + 2e^- \rightarrow H_2O}$

Overall: $\mathrm{CO + {}^1\!/_2\, O_2 \rightarrow CO_2}$

In this paper, first, the promising electrocatalysts that could effectively electrooxidize carbon monoxide are identified. Then, the catalysts and the ionomers are developed and the MEAs are fabricated. Finally, the manufactured single fuel cells are tested and the results are presented.

In this work, for the preparation of the anodic electrocatalysts, the metal precursors were separately dissolved in Ethylene Glycol, and then the solutions were mixed. The KOH solution was added to the mixture while it was stirred constantly. The catalyst was synthesized by the subsequent reduction process after the addition of $NaBH_4$ in the H_2O-ethylene glycol solvent. Finally, the solid catalyst particles were filtered, washed, and dried. Depending on whether the catalyst was carbon-supported or not, Vulcan could be added to the anodic catalyst. For creating the anodic catalyst solution (ink), the supported or unsupported anode catalyst powder was mixed with Nafion® solution and water. For the cathode catalyst ink, Pt black was mixed with Nafion® solution and water. The inks were painted on the surfaces of two pieces of carbon paper. In all cases, the area of each carbon paper was 5 cm^2. The painted carbon papers were dried and then hot-pressed on opposite sides of a Nafion® membrane at a temperature of 140°C for six minutes. Nafion®117 by DuPont was used as the membrane. For electrode polyelectrolyte bindings, D521 and D1021 Nafion® dispersions (from Ion Power Inc.) were used as the binders.

After each fuel cell was made, it was tested using a fuel cell test station, an 850e Fuel Cell Test System manufactured by a company named Scribner. The test station and its components are fully controlled by a computer and are designed to test both stack and single PEMFCs and DMFCs. The system is equipped with variable temperature humidifiers for both anode and cathode flows. The cell operating temperature and the mass flow rates of both anode and cathode can be also controlled. A wide variety of gases can be fed to the anode and cathode. After the single cell is connected to the test station and all operating conditions are fixed, the polarization curve for the cell is automatically generated by the system.

To validate the procedure for the preparation of the custom-made electrocatalysts and MEAs, a commercial DMFC MEA was purchased and tested. Then, Pt-Ru electrocatalysts, both supported and unsupported, were developed and MEAs were manufactured according to the above procedure. A wide variety of experimentations were conducted to evaluate the impacts of cell temperature, different types of fuel and oxidant, the flow rate of fuel and oxidant, and humidification temperature on the performance of the MEAs. The results of the experiments on the commercial and homemade MEAs were compared in the following sections.

In the following sections, for simplification, the properties of MEAs might be shown as membrane/anode/cathode or anode/cathode. For example, a fuel cell made of platinum-ruthenium (Pt-Ru) as the anode electrocatalyst, platinum (Pt) as the cathode electrocatalyst, and Nafion® 117 as the electrolyte membrane may be identified as (N117/Pt-Ru/Pt) or (Pt-Ru/Pt). Also, 90/85/80°C indicates that the operating temperature of the MEA, the temperature of the anode humidification flow, and the temperature of the cathode humidification flow are 90, 85, and 80°C, respectively. Similarly, 100/200 mlit/min means the flow rates of the anode and cathode streams are 100 and 200 mlit/min, respectively.

3. RESULTS AND DISCUSSIONS

3.1. Platinum-Ruthenium (Pt-Ru) Catalysts

Pt-Ru alloys are the workhorse of PEM fuel cell anode catalysts whenever high-purity hydrogen is not available as fuel. The reported reason is that Ru partially inhibited the creation of chemisorbed CO species (Camara et al., 2004). Several papers provided detailed analyses of this phenomenon (Pasupathi & Tricoli, 2008; Antolini, 2007). Many papers have been dedicated to the study of the performance of DMFCs and DEFCs when the anode catalyst was a Pt-Ru alloy (Poerwoprajitno et al., 2022; Luo et al., 2021; Wang et al., 2020b; Wang et al., 2020c; Spinacé et al., 2004a; Spinacé et al., 2004b; Choi et al., 2003; Fujiwara et al., 2002; Watanabe & Motoo, 1975) and many more using this type of catalyst as the benchmark for their cells (Colmati et al., 2006; Song et al., 2005; Neto et al., 2005; Lamy et al., 2004; Zhou et al., 2004; Reddington, 1998; Aramata & Masuda, 1991).

Schmidt et al. (1995) demonstrated that the CO tolerance of a PEMFC with a Pt-Ru anode catalyst is significantly improved compared to that of Pt/Vulcan anode catalysts. Later they reported similarly promising results for CO/H_2 gas mixture as the representation of the reformer gas (Schmidt et al., 1997b). Ren et al. (2000) studied many DMFCs with unsupported Pt-Ru anode catalysts and demonstrated the advantage of small particle sizes, which resulted in the high surface area of the catalysts. More recently, Li & Baek (2019) provided the latest advancement in the development of Pt and Ru-based electrocatalysts for the hydrogen evolution reaction.

Some researchers used nano-composite of Pt-Ru alloys (Wang et al., 2020d; Choi et al., 2003; Deivaraj & Lee, 2005). Deivaraja and Lee (2005) prepared carbon-supported Pt-Ru nanoparticles using three methods and compared their performance. They reported that all three catalysts were superior to the commercially available Pt catalysts. They demonstrated that the particle size (the mean diameter of the Pt-Ru nanoparticles) was affected by the fabrication method. However, the impact of a more homogenous alloy nanoparticle was more dominant in the electrochemical activity of the catalysts and their tolerance to carbon monoxide.

3.2. Performance of Commercial Dmfc Mea

The experiments were started by using a commercial direct methanol fuel cell made of carbon-supported platinum-ruthenium (Pt-Ru black) as the anode electrocatalyst, carbon-supported platinum (Pt black) as the cathode electrocatalyst, and Nafion® 117 as the electrolyte membrane. The loading of electrocatalysts for both the anode and cathode were 4 mg/cm^2. The surface area of the fuel cells in all experiments was 5 cm^2. The gas diffusion layers for the cathode and anode were made of ETEK ELAT® and carbon cloth, respectively.

First, the fuel cell was fed with hydrogen and oxygen as the fuel and oxidant, respectively. Then, the experiment was repeated by using a fuel composed of 20% CO and 80% N_2 (volume-based) and oxygen as an oxidant. In both cases, the operating temperature of the cell was 40°C. The difference between the maximum power densities in the two cases was staggering (277.7 vs. 11.6 mW/cm^2). This demonstrated that for an MEA that is not optimized for operation with carbon monoxide, in terms of both the fabrication process and operating conditions, the performance of the cell when fueled with H_2 and CO is not comparable.

To verify the consistency of the experimental procedure and to make sure that the results of the experiments are repeatable, the polarization curves of the fuel cell were obtained at various operating conditions. Fig. 2 shows the results for six experiments at three operating temperatures, 40, 60, and 100°C and two flow rates of 20/40 mlit/min and

100/100 mlit/min for the anode and cathode, respectively. The curves demonstrate that the repeatability of the results was acceptable and was within the experimental errors at the given operating temperatures and reactant flow rates. This observation is important because the fuel contains a high concentration of CO (20% CO and 80% N_2) in all cases. The diagrams in Fig. 2 also show that at high current densities the difference between curves slightly increases, particularly at low flow rates. However, even in these conditions, the results are reasonably close.

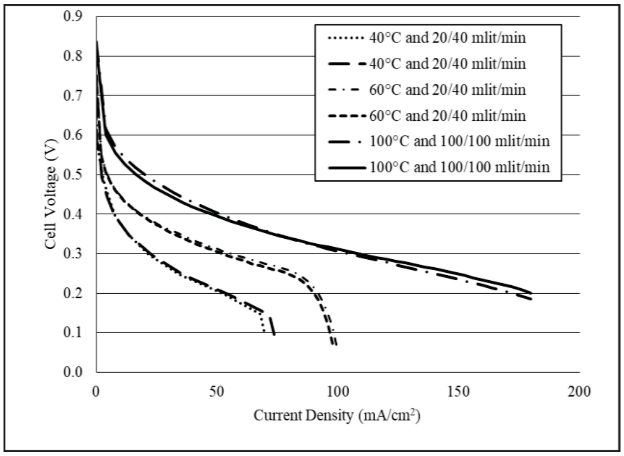

Fig. 2. The polarization curves of the commercial DMFC: The confirmation of the repeatability of the experiments (fuel: the mixture of 20% CO and 80% N_2, oxidant: O_2).

Next, the impact of the operating temperature on the polarization curve was investigated. Fig. 3 illustrates the polarization curves of the commercial DMFC for the operating temperatures of 40/40/30°C, 60/60/50°C, 80/75/75°C, and 100/95/90°C when fueled with the mixture of 20% CO and 80% N_2 (volume-based) and the oxidant of oxygen (at the flow rates of 20 and 80 mlit/min, respectively). As expected, increasing the operating temperature of the fuel cell improves its performance. The maximum power density increases from 10.8 to 26.6 mW/cm^2 when the operating temperature increases from 40 to 100°C. Similar consistent improvements can be seen at the operating temperatures of 60 and 80 °C with the maximum power densities of 20.7 and 24.6 mW/cm^2, respectively. These are moderate outputs that are partially due to the significant activation polarization losses. Using custom-synthesized catalysts should reduce these losses.

The only abnormal behavior in Fig. 3 is when the fuel cell operates at a high temperature (the solid line) and the high current density where the voltage abruptly drops. The reason for this drop is the low flow rate of the reactants which results in the starvation of the cell at the high current densities where the concentration overpotential is dominant. As it will be shown next (Fig. 4), when the flow rates are sufficiently high, this phenomenon will not occur.

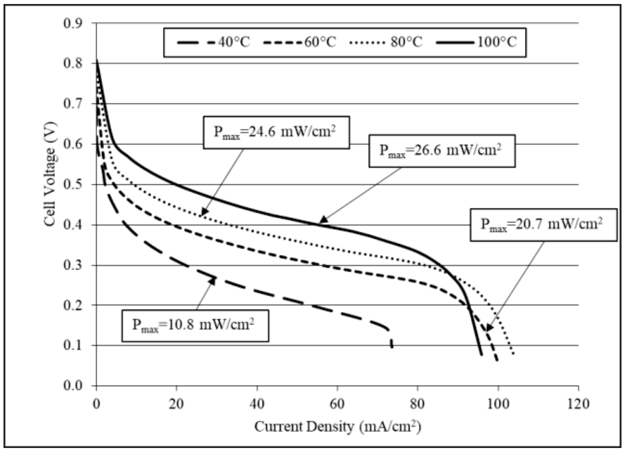

Fig. 3. The polarization curves of the commercial DMFC fed with the mixture of CO and N_2 as the fuel and oxygen as the oxidant (20/80 mlit/min): The effect of the cell operating temperature.

Fig. 4 illustrates the polarization curves of the same fuel cell operating at the temperature of 100/95/90°C with two flow rates, 20 and 100 mlit/min in the anode (20% CO and 80% N_2), and 40 and 100 mlit/min in the cathode (oxygen) (20/40 and 100/100 mlit/min). The curves indicate that at the high flow rates, the sudden voltage drop at the high current densities, observed in Fig. 3 due to cell starvation, was avoided.

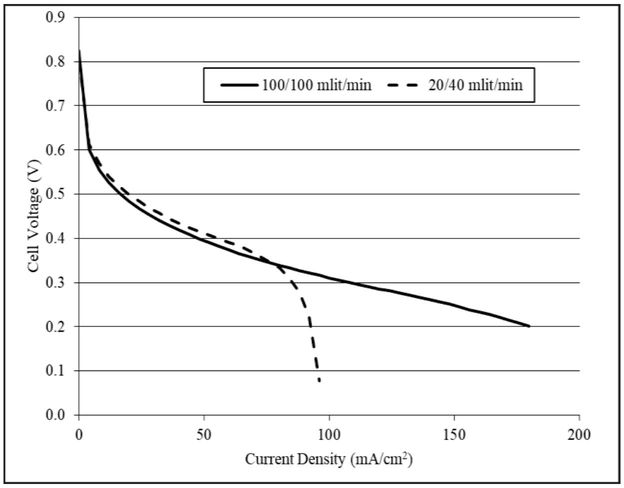

Fig. 4. The polarization curves of the commercial DMFC: The effect of the fuel and oxygen flow rates at the operating temperature of 95°C (20% CO and 80% N_2/O_2).

In the next set of experiments, the air is used as the oxidant instead of pure oxygen. First, the effect of the operating temperature of the cell on the polarization curve is investigated. Fig. 5 shows the polarization curves of the commercial DMFC when fueled with the mixture of 20% CO and 80% N_2 (volume-based) and air (at the flow rates of 20 and 80 mlit/min, respectively) for the operating temperatures of 40/35/35°C, 60/55/55°C, 80/75/75°C, and 100/95/95°C.

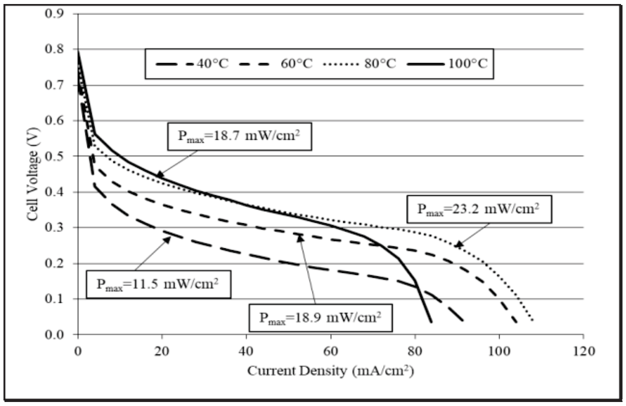

Fig. 5. The polarization curves of the commercial DMFC fed with the mixture of CO and N_2 (20 mlit/min) and air (80 mlit/min): The effect of the cell operating temperature.

The polarization curves in Fig. 5 indicate that the cell voltage is almost doubled when the operating temperature increases from 40 to 80°C. Similarly, the maximum power density is doubled, from 11.5 to 23.2 mW/cm^2. Comparing Fig. 5 and Fig. 3 indicates that the fuel cell performance, when fed with air or oxygen, was not significantly different. This result is expected because the electrochemical reactions in the anode are the limiting factor for the cell performance (refer to the discussion for Fig. 7). So, in this case, the type of oxidant flow does not make a major difference. It is however predicted that in the optimized MEA, the fuel cell fed with pure oxygen as the oxidant should outperform the one fed with air.

While there is no dramatic difference in the performance of the MEA when fed with air or oxygen, there are slight differences. At the operating temperatures of 60 and 80°C, the fuel cell fed with oxygen outperforms the one fed with air (Fig. 3 and Fig. 5). But at the operating temperature of 40°C, the fuel cell performance when fed with air is slightly better compared to that of the oxygen-fed fuel cell. At the operating temperature of 100°C, the difference is significant (the maximum power density of 26.6 mW/cm^2 for the oxygen-fed fuel cell compared to that of 18.7 mW/cm^2 for the air-fed fuel cell). Also, similar to the case with oxygen as the oxidant, at the operating temperature of 100°C, the voltage drops significantly at the high current densities compared to other operating temperatures. Again, the reason for both phenomena is the low flow rate of the reactants and the starvation of the fuel cell at the high current densities. Fig. 6 shows that increasing the flow rates of the reactants from 20/80 to 100/500 mlit/min prevents this phenomenon.

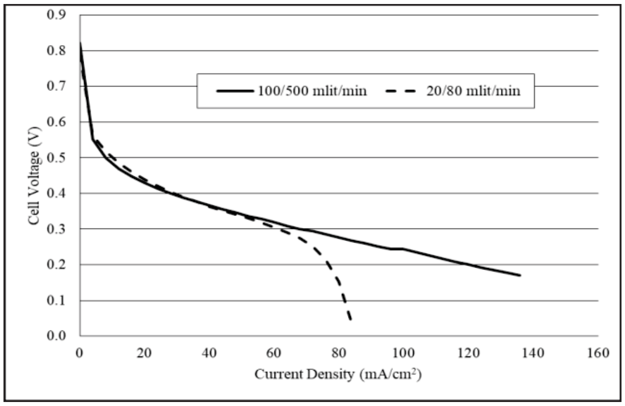

Fig. 6. The polarization curves of the commercial DMFC fed with the mixture of CO and N_2 as the fuel and air as the oxidant at the cell operating temperature of 100°C: The effects of flow rates of the reactants.

In the discussions for Fig. 3 and Fig. 5, it was explained that the electrochemical reactions in the anode are the limiting factor for the cell performance. The next step is to check this hypothesis by determining whether the impact of the flow rates of the reactants to the anode or the cathode is dominant in the performance of the fuel cell. Fig. 7 illustrates the polarization curves of the commercial DMFC at various anode and cathode flow rates at the cell operating temperature of 100°C.

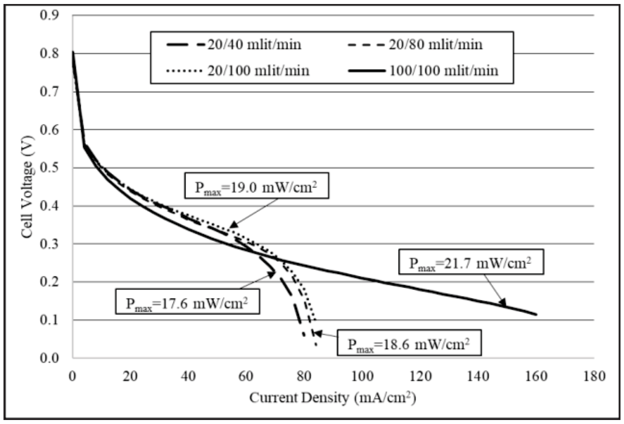

Fig. 7. The polarization curves of the commercial DMFC fed with the mixture of CO and N_2 and air at

the cell operating temperature of 100°C: The effects of flow rates of the reactants.

In three of the experiments, the fuel (a mixture of CO and N_2) flow rate was kept constant at 20 mlit/min and the flow rate of air was varied at 40, 80, and 100 mlit/min. The diagram indicates that the performance of the fuel cell is slightly improved with an increase in the flow rate of air (the maximum power density of the cell increases from 17.6 to 19.0 mW/cm^2 when the air flow rate increases from 40 to 100 mlit/min). In the two cases, the air flow rate was fixed at 100 mlit/min while the fuel flow rate was 20 and 100 mlit/min. This time the performance of the fuel cell improved by about 14% when the fuel flow rate increased. This confirms the fact that the anode is mainly limiting the performance of the fuel cell.

Finally, as the last experiment on the commercial DMFC, the effect of the fuel and air humidification temperatures on the performance of the fuel cell is investigated. For this purpose, the operating temperature of the cell was fixed at 80°C and the flow rates of the fuel (the mixture of CO and N_2) and air were 50/250 mlit/min and the humidification temperature was varied between 80 and 90°C with an increment of 5°C. The curves in Fig. 8 show that an increase in the humidification temperature (both the anode and the cathode) does not change the cell performance significantly and only a slight improvement is observed.

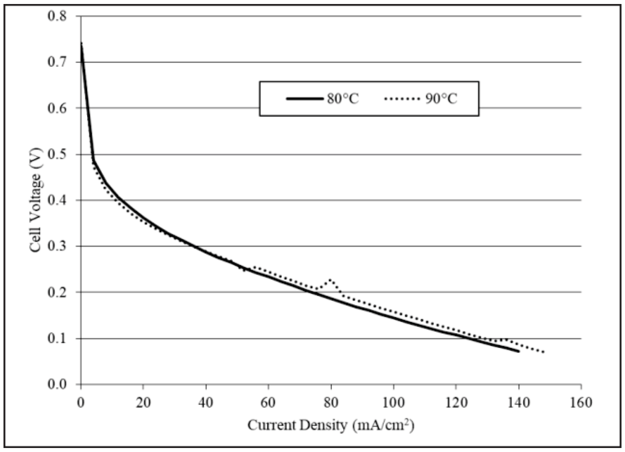

Fig. 8. The polarization curves of the commercial DMFC at the cell operating temperature of 80°C (CO+N_2/Air, 50/250 mlit/min): The effects of humidification temperature.

3.3. Repeatability of The Mea Fabrication Process

In order to make sure that the procedure to fabricate MEAs is repeatable, two MEAs were fabricated with the same procedure and parameters (as outlined previously) and then the results of the experiments were compared. The objective was to show that the developed fabrication procedure included all the important parameters and that there is no unknown parameter that may affect the results.

For this purpose, two MEAs were fabricated with the same procedure and were tested under the same operating conditions. The anode electrocatalyst of the fabricated MEAs was unsupported Pt-Ru with a platinum loading of 6 mg/cm^2 and the cathode electrocatalyst was the carbon-supported platinum with a loading of 4 mg/cm^2. The electrolyte membrane was Nafion® 117. It has been reported that the atomic ratio of 1:1 provides the optimum performance (Matsui et al., 2006; Oetjen et al., 1996; Watanabe & Motoo, 1975); therefore, this ratio was used.

Fig. 9 illustrates the polarization curve of the two MEAs when they were fed with CO as the fuel and oxygen as the oxidant with the mass flow rates of 100 and 200 mlit/min, respectively. The two fuel cells were tested at extreme temperatures of 40 and 95°C. The diagrams show that at the low temperature, the performance of the cells is reasonably close. For the high temperature, at the low and intermediate current densities, the curves are close, but at the high current densities, there are some discrepancies. Interestingly, however, the same irregularities occur in both cells, although not always at the same current density. Overall, these experiments prove that both the test procedure and MEA fabrication procedure are reasonably repeatable.

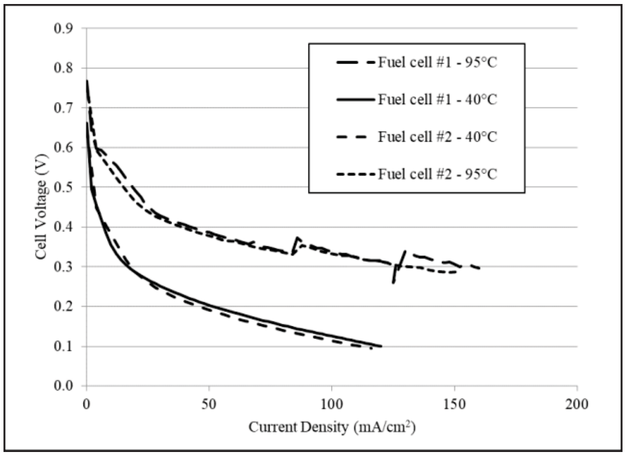

Fig. 9. The polarization curves of the Pt-Ru/Pt MEA: The repeatability of the test and fabrication procedures (CO/O_2 - 100/200 mlit/min).

3.4. Performance of Homemade Pt-Ru Catalyst

The unsupported Pt-Ru electrocatalyst and the MEA were fabricated according to the procedure explained before with the catalyst loading of 6 mg/cm^2 in the anode. The cathode electrocatalyst was the carbon-supported platinum with the loading of 4 mg/cm^2. The electrolyte membrane was Nafion® 117. Fig. 10

illustrates the effect of the cell operating temperature on the performance of the single Pt-Ru/Pt fuel cell when it was fueled with carbon monoxide and oxygen (flow rates 25 and 50 mlit/min, respectively). It should be noted that in these tests the temperatures of the fuel and oxidant humidifiers were set equal to the temperature of the cell. This will be the case for all experiments unless stated otherwise. As expected, the performance of the single fuel cell is improved at high temperatures. The maximum power density of 33.8 mW/cm^2 is achieved at the current density of about 200 mA/cm^2 for the operating temperature of 80°C followed by 21.1 mW/cm^2 at 140 mA/cm^2 and 11.8 mW/cm^2 at 95 mA/cm^2 at the temperatures of 60 and 40°C, respectively. The open-circuit voltage of the single cells for 80, 60, and 40°C are 0.708, 0.666, and 0.653 V, respectively. This strong dependency of the performance of the fuel cell on the operating temperature is expected (Anil & Madras, 2020; Antolini, 2007). Lee et al. (2004) demonstrated that the performance improvement of DMFCs at high temperatures was significantly higher for the carbon-supported Pt-Ru anode catalyst compared to that of the carbon-supported Pt. Similarly, Colmati et al. (2006) compared two anode catalysts for DMFCs, the carbon-supported Pt and the carbon-supported Pt–Ru. They demonstrated that the rate of improvement in the maximum power density as a function of the operating temperature is much higher for the carbon-supported Pt–Ru catalyst.

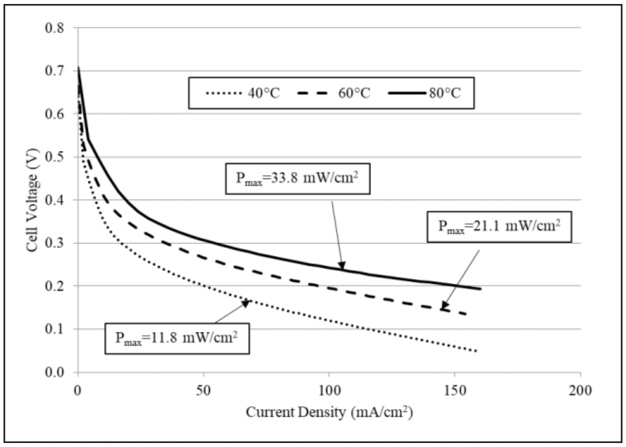

Fig. 10. The polarization curves of Pt-Ru MEA: The effect of the cell operating temperature (fed with CO/O$_2$ - 25/50 mlit/min).

The same pattern can be seen when the carbon monoxide and oxygen flow rates of the same fuel cell were increased to 100 and 200 mlit/min, respectively, and the cell operating temperature varied from 40 to 95°C (Fig. 11). The curves show that at the operating temperatures of 80 and 95°C some irregularities can be observed at the intermediate and high current densities. In this case, the maximum power density for operating temperatures of 95, 80, 60, and 40°C were 58.7, 33.2, 19.5, and 12.5 mW/cm^2, respectively. Interestingly, for the operating temperatures of 80 and 60°C the maximum power densities are slightly decreased in Fig. 11 (33.2 and 19.5 mW/cm^2, respectively) compared to Fig. 10 (33.8 and 21.1 mW/cm^2, respectively).

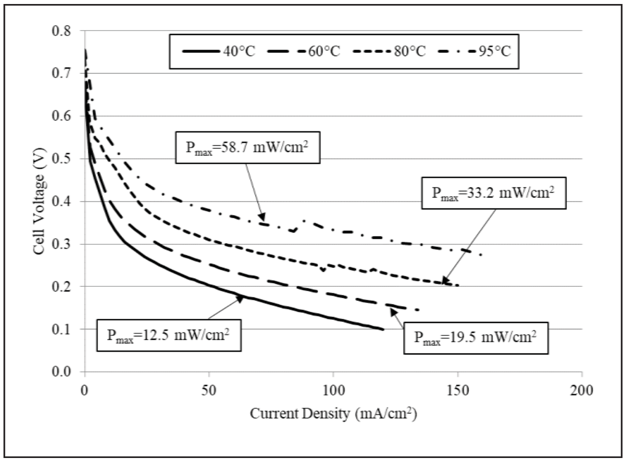

Fig. 11. The polarization curves of the Pt-Ru MEA: The effect of the cell operating temperature (fed with CO/O$_2$ - 100/200 mlit/min).

The influence of the fuel and oxidant flow rates is investigated in Fig. 12. The figure shows the polarization curves of the single fuel cell fed with carbon monoxide/oxygen at the flow rates of 25/50 and 100/200 mlit/min at the operating temperatures of 80, 60, and 40°C. The diagram shows that while there are slight variations, the impact of the fuel and oxidant flow rates (CO and O$_2$, respectively) at various operating temperatures is not significant.

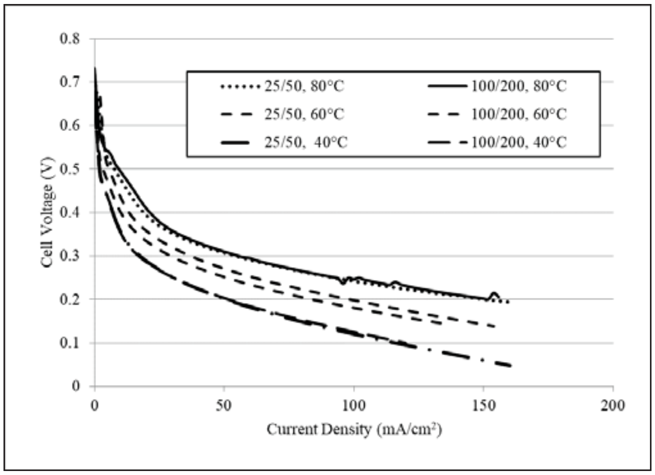

Fig. 12. The polarization curves of Pt-Ru MEA: The effect of the fuel (CO) and the oxidant (O$_2$) flow rates.

The experiment was repeated by using hydrogen as the fuel. Fig. 13 illustrates the polarization curves of the fuel cell when it was fueled with hydrogen and oxygen (flow rates 50/50 and 100/200 mlit/min) at the operating temperature of 40°C. As the figure shows, the performance of the fuel cell is slightly improved with an increase in the flow rates of the fuel and the oxidant (the maximum power densities 197 and 208 mW/cm^2, respectively).

To further investigate the effect of the flow rates of the fuel, the same cell was tested using the mixture of 20% carbon monoxide and 80% nitrogen as the fuel and oxygen as the oxidant at the operating temperature of 95°C when the flow rates are 500/1000, 100/200, and 25/50 mlit/min. Fig. 14 shows that with this fuel at low current densities (less than 30 mA/cm^2), the change in the performance of the fuel cell as a result of different reactant flow rates is small. But at the intermediate and high current densities, the performance of the cell quickly deteriorates at the low flow rates, i.e. 100/200 and 25/50 mlit/min. The reason is that with the low fraction of carbon monoxide in the fuel, the concentration loss quickly becomes the dominant loss due to the low partial pressure of CO in the triple-phase boundary (TPB) and the fuel starvation of the cell.

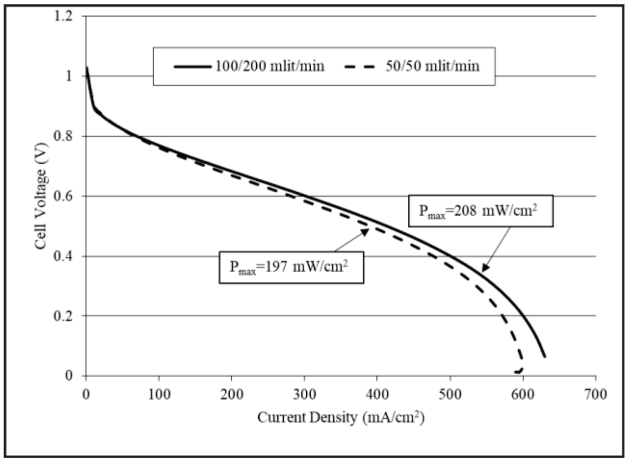

Fig. 13. The polarization curves of Pt-Ru MEA: Effect of the fuel and oxidant (H_2/O_2) flow rates at the operating temperature of 40°C.

As Fig. 14 indicates, this phenomenon cannot be seen for the entire range of current density at the high flow rates (500/1000 mlit/min), for current densities lower than 130 mA/cm^2 at the intermediate flow rates (100/200 mlit/min), and current densities lower than 30 mA/cm^2 at the low flow rates (25/50 mlit/min) because at these conditions there are plenty enough fuel to push the reactions forward. Furthermore, the fuel cell was tested when either air or oxygen was used as the oxidant (Fig. 15). In these tests, a mixture of 20% CO and 80% N_2 was used as the fuel. For both cases, the operating temperature of the cell was 95°C. As expected, the performance of the fuel cell when oxygen was used as the oxidant is better than that of the air. However, the difference is not significant because, as noted earlier, the reaction in the cathode is not a major limiting factor for the overall performance of the cell. Also, the irregularities in the curves are due to the high operating temperature of the cell. Next, the fuel cell was fueled with 100% carbon monoxide and the mixture of 20% CO and 80% N_2 (volume-based) and was tested. In both cases, the operating temperature was fixed at 95°C, the fuel flow rate at 100 mlit/min, and the oxygen flow rate at 200 mlit/min.

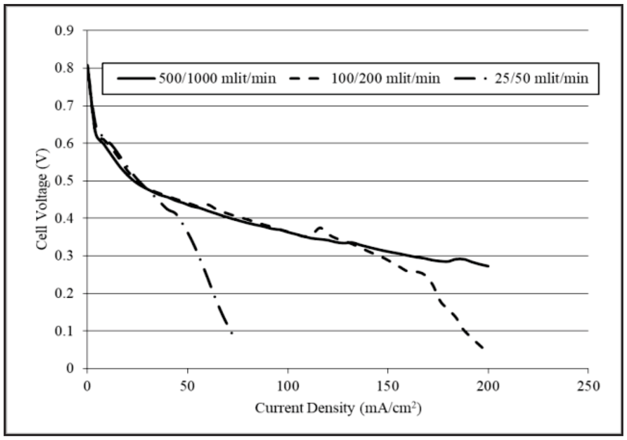

Fig. 14. The polarization curves of Pt-Ru MEA: The effect of the fuel and oxidant (20% CO and 80% N_2/O_2) flow rates at the operating temperature of 95°C.

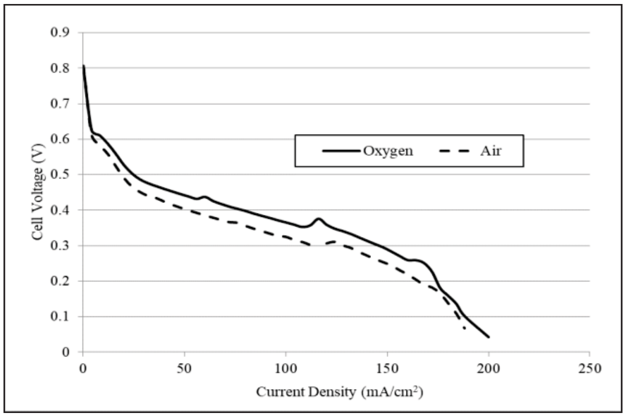

Fig. 15. The polarization curves of Pt-Ru MEA: The effect of the type of the oxidant gas, i.e. air and oxygen (the mixture of 20% CO and 80% N_2 as the fuel for both cases) at the operating temperature of 95°C.

The polarization curves shown in Fig. 16 indicate that the performance of the fuel cell in two cases is close at the low current densities (less than 130 mA/cm^2), but at high current densities, the fuel cell fueled with pure CO outperforms the other fuel (the maximum power densities of 55.5 and 42.4 mW/cm^2, respectively). The reason is that when the fuel cell was fed with the mixture of CO and N_2, it was starved of the fuel in the anode at high current densities due to the low concentration of CO. Similar to Fig. 14, the high operating temperature of the cell caused some irregularities in the curves.

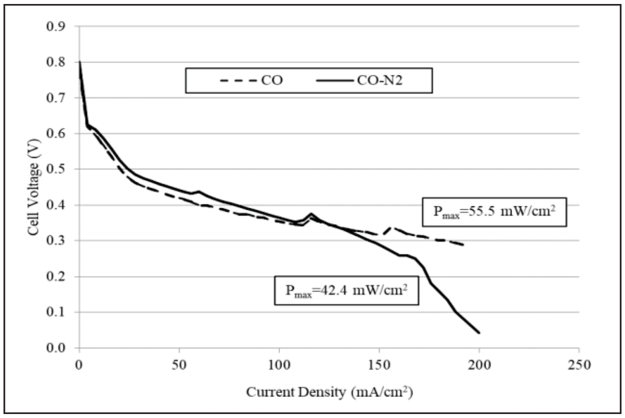

Fig. 16. The polarization curves of Pt-Ru MEA at the operating temperature of 95°C with the fuel flow rate of 100 mlit/min and the oxygen flow rate of 200 mlit/min: The effect of the fuel type (CO vs. the mixture of CO-N_2).

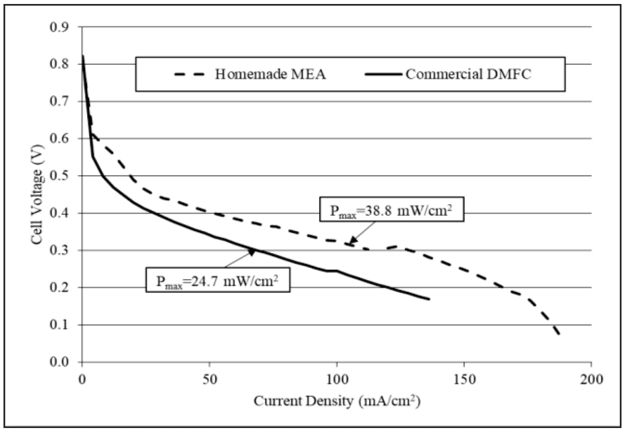

Fig. 17. The polarization curves of the homemade Pt-Ru MEA and the commercial DMFC when fueled with the mixture of CO and N_2 as the fuel and air as the oxidant (100/500 mlit/min) at the operating temperature of 95°C.

To evaluate the quality of the MEA fabrication process used to make the MEAs, the polarization curves of the homemade fuel cells were compared to that of the commercial DMFC. Fig. 17 indicates that the performance of the homemade MEA is better than that of the commercial fuel cell when they are fueled with a mixture of CO-N_2 and air (100/500 mlit/min) at the operating temperature of 95°C (the maximum power density of 38.8 vs 24.7 mW/cm^2, respectively). The reason might be the slightly higher anode platinum loading of the homemade MEA compared to that of the commercial one. Similar to Fig. 17, the polarization curves in Fig. 18 compare the two homemade and commercial MEAs; this time when fueled with hydrogen and air (100/200 mlit/min) at the operating temperature of 40°C. Interestingly, in this case, the commercial MEA outperformed the homemade one (the maximum power density of 278 vs. 208 mW/cm^2, respectively) which is contrary to the trend for MEAs when fueled with CO-N_2 (Fig. 17).

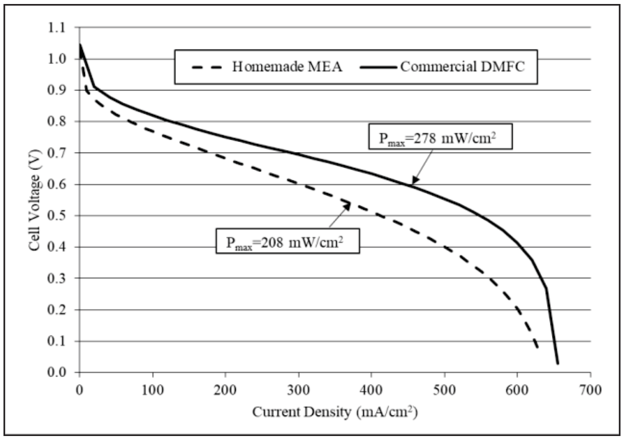

Fig. 18. The polarization curves of the homemade Pt-Ru MEA and the commercial DMFC when fueled with hydrogen and air at the operating temperature of 40°C (100/200 mlit/min)

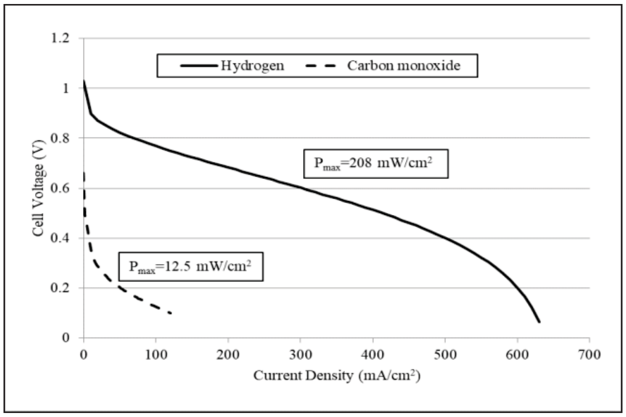

Fig. 19. The polarization curves of Pt-Ru MEA: The effect of the fuel type; hydrogen vs. carbon monoxide (oxygen as the oxidant) at the operating temperature of 40°C (hydrogen and carbon monoxide flow rates 100 mlit/min and oxygen flow rate 200 mlit/min).

The reason is that in this case (H_2-fueled MEA), the commercial MEA contained plenty of catalyst (platinum) particles for hydrogen oxidation and the slightly more platinum loading in the homemade MEA did not make any meaningful difference. In the meantime, the higher quality of the fabrication of the commercial MEA provided it with better performance at similar operating conditions. Finally, the performance of the single fuel cell fueled with various fuels was investigated. The impact of using carbon monoxide and the mixture of carbon monoxide and nitrogen was already discussed in Fig. 16. Here the performance of the fuel cell fueled with carbon monoxide and hydrogen was compared (Fig. 19). The hydrogen and carbon monoxide flow rates were 100 mlit/min and the oxygen flow rate was 200 mlit/min. The operating temperature of the cell was fixed at 40°C. The maximum power densities of the cell when fueled with hydrogen and carbon monoxide were 208 mW/cm^2 at 450 mA/cm^2 and 12.5 mW/cm^2 at 80 mA/cm^2, respectively (almost 16.6 times lower maximum power density for the latter). This inferior performance of the cell when fueled with CO is not acceptable and new material and optimized operating conditions should be sought.

As noted earlier, the catalytic activity of an electrocatalyst depends on the characteristics of both the metallic catalyst and its support. Furthermore, the size distribution of catalyst particles and their dispersion through electrodes can significantly impact the catalytic activity (Goel & Basu, 2012). In the next section, the effects of using different catalyst support materials on the performance of the Pt-Ru catalyst will be investigated.

3.5. Carbon-Supported Pt-Ru (Pt-Ru/Vulcan)

Electrodes in PEMFCs have three major functions:

- to provide sites for electrochemical reactions of fuel and oxidant at the triple-phase boundary (TPB), which require high catalytic activity,
- to conduct electrons and ions to and from the TPB, which require high ionic and electronic conductivities,
- to provide a path for the flow of reactants to the TPB and the flow of products from the TPB, which require high porosity.

In many catalysts, a support material with a high surface area and high conductivity is added to improve the electrical conductivity of the catalyst. Catalyst supports function as the connecting agent between the catalyst and the porous backing. Moreover, they can decrease the usage of expensive noble metals, increase surface area, improve catalytic activity, increase porosity, and reduce the degradation of metal catalysts (Choi et al., 2003). Carbon particles have been the most common catalyst support material though other materials, such as conducting polymers (e.g., Polyaniline), have also been proposed and used due to their high electronic conductivity, stability, and surface area (Choi et al., 2005). Carbon nanotubes (CNTs) have recently become popular to be used as carbon support in electrocatalysts because of their extraordinary electrical, chemical, mechanical, and thermal characteristics, particularly their high surface-to-volume ratio (Lilloja et al., 2021; Devrim & Arıca, 2020; Mohideen et al., 2020; Fard et al., 2020; Wang et al., 2020d; Antolini, 2007; Matsumoto et al., 2004; Coq et al., 1998). Similarly, multi-walled carbon nanotubes (MWNTs) have attracted some attention as the superior carbon support for electrocatalysts (Wang et al., 2023; Bekmezci et al., 2023; Yang et al., 2019; Xu et al., 2006; Wu et al., 2005; Li et al., 2003). However, the most popular type of carbon support material for PEMFCs is still Vulcan XC-72 carbon black (Şahin et al., 2023; Alawadhi et al., 2020; Sapkota et al., 2022; Liu et al., 2004; Matsumoto et al., 2004; Bock et al., 2004).

Devrim & Arıca (2020) investigated three support materials used in catalysts for high-temperature PEMFCs, Pt/C, Pt/CNT, and Pt/GCNT (graphitized CNT). They showed that Pt/GCNT and Pt/CNT had superior performance compared to that of Pt/C. Goel et al. (2012) compared the performance of a DEFC with the anode catalyst made of Pt-Re-Sn with two support materials, multi-walled carbon nanotubes and Vulcan-XC. They showed that the performance of the fuel cell with multi-walled carbon nanotubes as the support was superior to that of the Vulcan-XC as the support.

The fabrication process for the MEA in this section was exactly similar to the process used for the previous MEAs. The anode electrode of the fabricated MEA was the carbon-supported Pt-Ru with the platinum loading of 6 mg/cm^2 and the cathode electrode was the carbon-supported platinum with the loading of 4 mg/cm^2 and Nafion® 117 as the electrolyte.

To compare a carbon-supported MEA and an unsupported MEA, the two MEAs were tested in similar operational conditions. Fig. 20 shows the maximum power densities of the carbon-supported MEA when it was fueled with 100% CO and oxygen as the oxidizer (with the flow rates of 100 and 200 mlit/min, respectively) at the operating temperatures of 80 and 95°C were 12.6 and 18.1 mW/cm^2, respectively. The maximum power densities of the unsupported MEA at similar operating conditions were 33.2 and 58.7 mW/cm^2, respectively (Fig. 11). Similar experiments using hydrogen as the fuel showed similar results. This indicates that the addition of carbon support significantly deteriorated the performance of the MEA in these cases. However, the figure indicates that with only a 15°C increase in the operating temperature, the performance of the cell significantly improves.

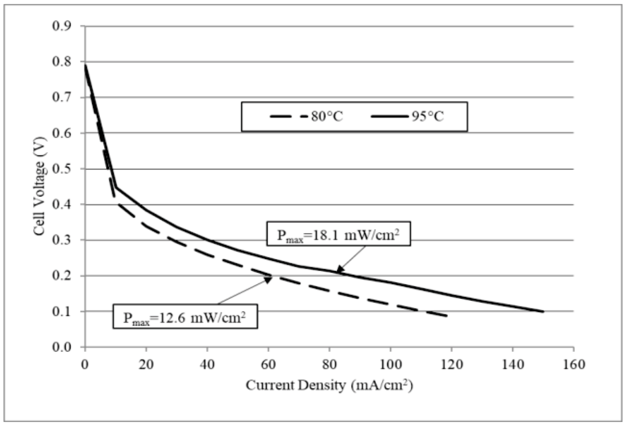

Fig. 20. The polarization curves of the carbon-supported Pt-Ru MEA fed with carbon monoxide and oxygen (100/200 mlit/min): The effect of the operating temperature.

To determine if the performance of the cell can be improved by optimizing the operating conditions, several experiments were conducted. Fig. 20 shows that increasing the operating temperature of the fuel cell from 80 to 95°C improved the maximum power density by about 44%. Fig. 21 illustrates the polarization curves of the fuel cell when fueled with CO and O_2 at the operating temperature of 95°C for the different flow rates of carbon monoxide and oxygen. Four different flow rates were examined: 100/200, 250/500, 500/100, and 1000/2000 mlit/min. The figure shows that the four curves are very close and indicates that the effects of the flow rates, both fuel and oxidant, are not significant.

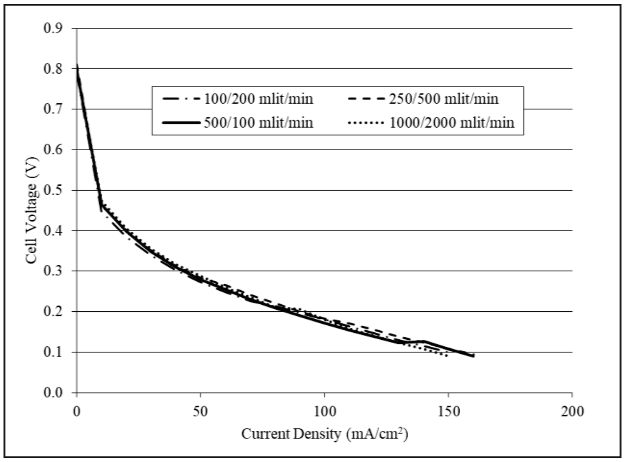

Fig. 21. The polarization curves of the carbon-supported Pt-Ru MEA fed with carbon monoxide and oxygen at the operating temperature of 95°C: The effect of the fuel and the oxidant flow rates.

Fig. 22 shows the impact of the anode and cathode humidification temperatures on the performance of the fuel cell in two cases, when the fuel cell was fueled with hydrogen and when it was fueled with carbon monoxide (both with a flow rate of 100 mlit/min). In these experiments, the oxidant was oxygen (with a flow rate of 200 mlit/min) and the fuel cell operating temperature was 80°C. In each experiment, the anode and cathode humidification temperatures were equal and varied between 75 and 80°C. Surprisingly, the performance of the fuel cell improved markedly with only a 5°C increase in the humidification temperatures. In the case of the hydrogen-fueled MEA, the maximum power density improved by about 10% (from 177 to 194 mW/cm^2), and in the case of the carbon monoxide-fueled MEA, by about 21% (from 10.4 to 12.6 mW/cm^2).

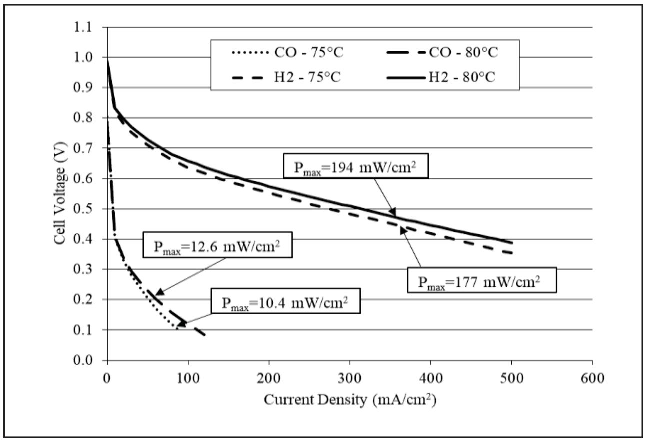

Fig. 22. The polarization curves of the carbon-supported Pt-Ru MEA fed with carbon monoxide and hydrogen as the fuel and oxygen as the oxidant (with flow rates of 100/200 mlit/min) at the operating temperature of 80°C: The effect of the anode and cathode humidification temperatures.

The results of experiments on the carbon-supported MEA indicate that it cannot compete with the unsupported MEA. Liu et al. (1998) reported that while supported catalysts showed better specific activities compared to that of the unsupported catalysts, they demonstrated no performance improvements when used as the anode catalysts in DMFCs. So, the results of these experiments may not be as unusual as they may seem.

4. CONCLUSION

As the first step for the development of DCMFCs and inspired by the vast literature on DAFCs, various Pt-Ru catalysts and MEAs were developed and examined. While the performance of these cells when fueled by CO and CO-containing fuels was markedly inferior to that of hydrogen-fueled cells, they showed some promising signs that with the right catalysts and optimum operating conditions, the performance of DCMFC can be significantly improved. More specifically the following conclusions can be made from the presented experimental results:

- The experimentations with the commercial DMFCs made of the Pt-Ru anode catalyst verified the repeatability of the experimental method. The results of the experiments were also used as a benchmark to confirm the repeatability of the anode electrocatalysts and MEAs fabrication methods.
- The results of the tests on the commercial and homemade Pt-Ru MEAs indicated that while the hydrogen-fueled commercial MEA outperformed the homemade one, the trend was reversed when the cell was fueled with CO-containing fuels.
- In all the MEAs, increasing the operating temperature improved the performance albeit with a different magnitude of improvement.
- Increasing the flow rates of the reactants improved the performancie of the MEAs up to a certain level and beyond that, the impact was not significant.
- Typically, the performance of the MEAs was better when fed with CO rather than CO-N_2 and O_2 rather than air but the actual impacts depended on other operating conditions.
- For the Pt-Ru anode electrocatalyst, using carbon (both Vulcan and carbon nanotubes) as the support for the anode catalyst proved to be fruitless and deteriorated the performance of the MEA.

Generally, the results for unsupported- and supported-Pt-Ru anode catalysts indicate that although the performance of the fuel cells can be improved significantly, still they are not at an acceptable level. Furthermore, ruthenium is a rare transition metal in the platinum group with very limited annual global production, and its utilization in the fuel cell fabrication should be reduced. Therefore, other binary, ternary, and quaternary alloys of platinum should be investigated.

5. ACKNOWLEDGEMENT

The authors would like to thank the American Science and Technology Corporation (AST) for sharing some of the data used in this paper.

REFERENCES

Alawadhi, H., Abdelkareem, M. A., Hussain, N., Wilberforce, T., and Sayed, E. T. (2020). A composite of graphitic carbon nitride and Vulcan carbon as an effective catalyst support for Ni in direct urea fuel cells. Journal of the Taiwan Institute of Chemical Engineers, 116, 160-168.

Alias, M. S., Kamarudin, S. K., Zainoodin, A. M., and Masdar, M. S. (2020). Active direct methanol fuel cell: An overview. International Journal of Hydrogen Energy, 45(38), 19620-19641.

Anil, C., and Madras, G. (2020). Catalytic behaviour of Mn2. 94M0. 06O4-δ (M= Pt, Ru and Pd) catalysts for low temperature water gas shift (WGS) and CO oxidation. International Journal of Hydrogen Energy, 45(17), 10461-10474.

Antolini, E. (2007). Catalysts for direct ethanol fuel cells. Journal of Power Sources, 170(1), 1-12.

Aramata, A., and Masuda, M. (1991). Platinum Alloy Electrodes Bonded to Solid Polymer Electrolyte for Enhancement of Methanol Electro-oxidation and Its Reaction Mechanism. Journal of The Electrochemical Society, 138(7), 1949-1957.

Bekmezci, M., Gules, G. N., Bayat, R., and Sen, F. (2023). Modification of multi-walled carbon nanotubes with platinum–osmium to develop stable catalysts for direct methanol fuel cells. Analytical Methods, 15(9), 1223-1229.

Bıyıkoğlu, A. (2005). Review of proton exchange membrane fuel cell models. International Journal of Hydrogen Energy, 30(11), 1181-1212.

Bock, C., Paquet, C., Couillard, M., Botton, G. A., and MacDougall, B. R. (2004). Size-selected synthesis of PtRu nano-catalysts: reaction and size control mechanism. Journal of the American Chemical Society, 126(25), 8028-8037.

Camara, G. A., De Lima, R. B., and Iwasita, T. (2004). Catalysis of ethanol electrooxidation by PtRu: the influence of catalyst composition. Electrochemistry Communications, 6(8), 812-815.

Cao, D., Sun, Y., and Wang, G. (2007). Direct carbon fuel cell: fundamentals and recent developments. Journal of Power Sources, 167(2), 250-257.

Choi, J. H., Park, K. W., Lee, H. K., Kim, Y. M., Lee, J. S., and Sung, Y. E. (2003). Nano-composite of PtRu alloy electrocatalyst and electronically conducting polymer for use as the anode in a direct methanol fuel cell. Electrochimica acta, 48(19), 2781-2789.

Choi, J. H., Kim, Y. M., Lee, J. S., Cho, K. Y., Jung, H. Y., Park, J. K., ... and Sung, Y. E. (2005). A polyaniline supported PtRu nanocomposite anode and a Pd-impregnated nanocomposite Nafion membrane for DMFCs. Solid State Ionics, 176(39), 3031-3034.

Clean Coal Research, http://energy.gov/fe/science-innovation/clean-coal-research, retrieved in July 2023.

Colmati, F., Antolini, E., and Gonzalez, E. R. (2006). Effect of temperature on the mechanism of ethanol oxidation on carbon supported Pt, PtRu and Pt 3 Sn electrocatalysts. Journal of Power Sources, 157(1), 98-103.

Coq, B., Planeix, J. M., and Brotons, V. (1998). Fullerene-based materials as new support media in heterogeneous catalysis by metals. Applied Catalysis A: General, 173(2), 175-183.

Deivaraj, T. C., and Lee, J. Y. (2005). Preparation of carbon-supported PtRu nanoparticles for direct methanol fuel cell applications–a comparative study. Journal of Power Sources, 142(1), 43-49.

Devrim, Y., and Arıca, E. D. (2020). Investigation of the effect of graphitized carbon nanotube catalyst support for high temperature PEM fuel cells. International Journal of Hydrogen Energy, 45(5), 3609-3617.

Fard, H. F., Khodaverdi, M., Pourfayaz, F., and Ahmadi, M. H. (2020). Application of N-doped carbon nanotube-supported Pt-Ru as electrocatalyst layer in passive direct methanol fuel cell. International Journal of Hydrogen Energy, 45(46), 25307-25316.

Fujiwara, N., Yasuda, K., Ioroi, T., Siroma, Z., and Miyazaki, Y. (2002). Preparation of platinum–ruthenium onto solid polymer electrolyte membrane and the application to a DMFC anode. Electrochimica Acta, 47(25), 4079-4084.

Goel, J., and Basu, S. (2012). Pt-Re-Sn as metal catalysts for electro-oxidation of ethanol in direct ethanol fuel cell. Energy Procedia, 28, 66-77.

Gottesfeld, S., and Pafford, J. (1988). A new approach to the problem of carbon monoxide poisoning in fuel cells operating at low temperatures. Journal of the Electrochemical Society, 135(10), 2651-2652.

Haider, R., Wen, Y., Ma, Z. F., Wilkinson, D. P., Zhang, L., Yuan, X., ... and Zhang, J. (2021). High temperature proton exchange membrane fuel cells: progress in advanced materials and key technologies. Chemical Society Reviews, 50(2), 1138-1187.

Hamnett, A. (1997). Mechanism and electrocatalysis in the direct methanol fuel cell. Catalysis Today, 38(4), 445-457.

Jiang, C., Ma, J., Corre, G., Jain, S. L., and Irvine, J. T. (2017). Challenges in developing direct carbon fuel cells. Chemical Society Reviews, 46(10), 2889-2912.

Lamy, C., Rousseau, S., Belgsir, E. M., Coutanceau, C., and Léger, J. M. (2004). Recent progress in the direct ethanol fuel cell: development of new platinum–tin electrocatalysts. Electrochimica Acta, 49(22), 3901-3908.

Lee, C.G., Umeda, M., Uchida, I. (2004) Temperature effect on methanol and ethanol electro-oxidation at Pt/C and Pt–Ru/C microporous electrodes, in: Electrochemical Society Meeting Abstracts, 206th Meeting, Honolulu, Hawaii.

Li, W., Liang, C., Zhou, W., Qiu, J., Zhou, Z., Sun, G., and Xin, Q. (2003). Preparation and characterization of multiwalled carbon nanotube-supported platinum for cathode catalysts of direct methanol fuel cells. The Journal of Physical Chemistry B, 107(26), 6292-6299.

Li, C., and Baek, J. B. (2019). Recent advances in noble metal (Pt, Ru, and Ir)-based electrocatalysts for efficient hydrogen evolution reaction. ACS omega, 5(1), 31-40.

Lilloja, J., Kibena-Põldsepp, E., Sarapuu, A., Douglin, J. C., Käärik, M., Kozlova, J., ... and Tammeveski, K. (2021). Transition-metal-and nitrogen-doped carbide-derived carbon/carbon nanotube composites as cathode catalysts for anion-exchange membrane fuel cells. Acs Catalysis, 11(4), 1920-1931.

Liu, L., Pu, C., Viswanathan, R., Fan, Q., Liu, R., & Smotkin, E. S. (1998). Carbon supported and unsupported Pt–Ru anodes for liquid feed direct methanol fuel cells. Electrochimica Acta, 43(24), 3657-3663.

Liu, Z., Ling, X. Y., Su, X., & Lee, J. Y. (2004). Carbon-supported Pt and PtRu nanoparticles as catalysts for a direct methanol fuel cell. The Journal of Physical Chemistry B, 108(24), 8234-8240.

Luo, M., Cai, J., Zou, J., Jiang, Z., Wang, G., & Kang, X. (2021). Promoted alkaline hydrogen evolution by an N-doped Pt–Ru single atom alloy. Journal of Materials Chemistry A, 9(26), 14941-14947.

Matsui, T., Fujiwara, K., Okanishi, T., Kikuchi, R., Takeguchi, T., & Eguchi, K. (2006). Electrochemical oxidation of CO over tin oxide supported platinum catalysts. Journal of power sources, 155(2), 152-156.

Matsumoto, T., Komatsu, T., Arai, K., Yamazaki, T., Kijima, M., Shimizu, H., ... and Nakamura, J. (2004). Reduction of Pt usage in fuel cell electrocatalysts with carbon nanotube electrodes. Chemical Communications, (7), 840-841.

Mohideen, M. M., Liu, Y., and Ramakrishna, S. (2020). Recent progress of carbon dots and carbon nanotubes applied in oxygen reduction reaction of fuel cell for transportation. Applied Energy, 257, 114027.

Neri, G., Arrigo, I., Corigliano, F., Espro, C., Galvagno, S., Modafferi, V., and Donato, A. (2014). Selective oxidation of CO in hydrogen atmosphere on Pt–Fe catalysts supported on zeolite P-based materials. Journal of Porous Materials, 21(5), 623-631.

Neto, A. O., Vasconcelos, T. R., Da Silva, R. W. R. V., Linardi, M., and Spinacé, E. V. (2005). Electro-oxidation of ethylene glycol on PtRu/C and PtSn/C electrocatalysts prepared by alcohol-reduction process. Journal of Applied Electrochemistry, 35(2), 193-198.

Oetjen, H. F., Schmidt, V. M., Stimming, U., and Trila, F. (1996). Performance data of a proton exchange membrane fuel cell using H_2/CO as fuel gas. Journal of the Electrochemical Society, 143(12), 3838-3842.

Ozalp, N., Abedini, H., Abuseada, M., Davis, R., Rutten, J., Verschoren, J., ... and Moens, D. (2022). An overview of direct carbon fuel cells and their promising potential on coupling with solar thermochemical carbon production. Renewable and Sustainable Energy Reviews, 162, 112427.

Pasupathi, S., and Tricoli, V. (2008). Effect of third metal on the electrocatalytic activity of PtRu/Vulcan for methanol electro-oxidation. Journal of Solid-State Electrochemistry, 12(9), 1093-1100.

Poerwoprajitno, A. R., Gloag, L., Watt, J., Cheong, S., Tan, X., Lei, H., ... and Tilley, R. D. (2022). A single-Pt-atom-on-Ru-nanoparticle electrocatalyst for CO-resilient methanol oxidation. Nature Catalysis, 5(3), 231-237.

Ramli, Z. A. C., Pasupuleti, J., Saharuddin, T. S. T., Yusoff, Y. N., Isahak, W. N. R. W., Baharudin, L., ... and Kiong, S. T. (2023). Electrocatalytic activities of platinum and palladium catalysts for enhancement of direct formic acid fuel cells: An updated progress. Alexandria Engineering Journal, 76, 701-733.

Reddington, E., Sapienza, A., Gurau, B., Viswanathan, R., Sarangapani, S., Smotkin, E. S., and Mallouk, T. E. (1998). Combinatorial electrochemistry: a highly parallel, optical screening method for discovery of better electrocatalysts. Science, 280(5370), 1735-1737.

Ren, X., Zelenay, P., Thomas, S., Davey, J., and Gottesfeld, S. (2000). Recent advances in direct methanol fuel cells at Los Alamos National Laboratory. Journal of Power Sources, 86(1), 111-116.

Şahin, Ö., Akdağ, A., Horoz, S., and Ekinci, A. (2023). Physical and electrochemical effect of bimetallic Pd–Mo nanoalloys supported on vulcan XC-72r carbon as cathode catalysts for proton exchange membrane fuel cell. Electrocatalysis, 14(2), 202-212.

Sapkota, P., Lim, S., and Aguey-Zinsou, K. F. (2022). Superior Performance of an Iron-Platinum/Vulcan Carbon Fuel Cell Catalyst. Catalysts, 12(11), 1369.

Schmidt, V. M., Ianneillo, R., Oetjen, H. F., Reger, H., Stimming, U., and Trila, F. (1995). Oxidation of H_2/CO in a proton exchange membrane fuel cell. In Proceedings of the First International Symposium on Proton Conducting Membrane Fuel Cells I (Vol. 95, p. 23). The Electrochemical Society: Pennington, NJ.

Schmidt, V. M., Oetjen, H. F., and Divisek, J. (1997a). Performance Improvement of a PEMFC Using Fuels with CO by Addition of Oxygen-Evolving Compounds. Journal of the Electrochemical Society, 144(9), L237-L238.

Schmidt, T. J., Noeske, M., Gasteiger, H. A., Behm, R. J., Britz, P., Brijoux, W., and Bönnemann, H. (1997b). Electrocatalytic activity of PtRu alloy colloids for CO and CO/H_2 electrooxidation: stripping voltammetry and rotating disk measurements. Langmuir, 13(10), 2591-2595.

Song, S. Q., Zhou, W. J., Zhou, Z. H., Jiang, L. H., Sun, G. Q., Xin, Q., … and Tsiakaras, P. (2005). Direct ethanol PEM fuel cells: the case of platinum-based anodes. International Journal of Hydrogen Energy, 30(9), 995-1001.

Spinacé, E. V., Neto, A. O., and Linardi, M. (2004a). Electro-oxidation of methanol and ethanol using PtRu/C electrocatalysts prepared by spontaneous deposition of platinum on carbon-supported ruthenium nanoparticles. Journal of Power Sources, 129(2), 121-126.

Spinacé, E. V., Neto, A. O., Vasconcelos, T. R., and Linardi, M. (2004b). Electro-oxidation of ethanol using PtRu/C electrocatalysts prepared by alcohol-reduction process. Journal of Power Sources, 137(1), 17-23.

Steele, B. C., and Heinzel, A. (2001). Materials for fuel-cell technologies. Nature, 414(6861), 345-352.

Wang, F., Deng, S., Zhang, H., Wang, J., Zhao, J., Miao, H., ... and Yan, J. (2020a). A comprehensive review on high-temperature fuel cells with carbon capture. Applied Energy, 275, 115342.

Wang, Q., Chen, S., Jiang, J., Liu, J., Deng, J., Ping, X., and Wei, Z. (2020b). Manipulating the surface composition of Pt–Ru bimetallic nanoparticles to control the methanol oxidation reaction pathway. Chemical Communications, 56(16), 2419-2422.

Wang, Y., Chen, Y., Zhang, L., Wang, G., Deng, W., and Guo, L. (2020c). Total catalytic oxidation of chlorinated aromatics over bimetallic Pt–Ru supported on hierarchical HZSM-5 zeolite. Microporous and Mesoporous Materials, 308, 110538.

Wang, M., Chen, D., Li, N., Xu, Q., Li, H., He, J., and Lu, J. (2020d). Highly efficient catalysts of bimetallic Pt–Ru nanocrystals supported on ordered ZrO_2 nanotube for toluene oxidation. ACS applied materials & interfaces, 12(12), 13781-13789.

Wang, J., Qu, T., Ni, J., Cheng, F., Hu, F., Ou, Y., ... and Liu, H. (2023). Composite proton exchange membranes based on inorganic proton conductor boron phosphate functionalized multi-walled carbon nanotubes and chitosan. Surfaces and Interfaces, 36, 102557.

Watanabe, M. A., and Motoo, S. (1975). Electrocatalysis by ad-atoms: Part II. Enhancement of the oxidation of methanol on platinum by ruthenium ad-atoms. Journal of Electroanalytical Chemistry and Interfacial Electrochemistry, 60(3), 267-273.

Wu, G., Chen, Y. S., and Xu, B. Q. (2005). Remarkable support effect of SWNTs in Pt catalyst for methanol electrooxidation. Electrochemistry Communications, 7(12), 1237-1243.

Xia, Z., Zhang, X., Sun, H., Wang, S., and Sun, G. (2019). Recent advances in multi-scale design and construction of materials for direct methanol fuel cells. Nano Energy, 65, 104048.

Xu, J., Hua, K., Sun, G., Wang, C., Lv, X., and Wang, Y. (2006). Electrooxidation of methanol on carbon nanotubes supported Pt–Fe alloy electrode. Electrochemistry communications, 8(6), 982-986.

Yang, J., Ganesan, P., Ishihara, A., and Nakashima, N. (2019). Carbon nanotube-based non-precious metal electrode catalysts for fuel cells, water splitting and zinc-air batteries. ChemCatChem, 11(24), 5929-5944.

Zabihian, F., Davari, A., and Osei-Prempeh, G. (2023). Carbon monoxide-resistant anode catalysts for single-cell direct carbon monoxide fuel cells (DCMFCs): Binary, ternary, and quaternary platinum alloys as anode electrocatalysts. International Journal of Renewable Energy Resources, In press.

Zheng, Y., Wan, X., Cheng, X., Cheng, K., Dai, Z., and Liu, Z. (2020). Advanced catalytic materials for ethanol oxidation in direct ethanol fuel cells. Catalysts, 10(2), 166.

Zhou, W. J., Li, W. Z., Song, S. Q., Zhou, Z. H., Jiang, L. H., Sun, G. Q., ... and Tsiakaras, P. (2004). Bi-and tri-metallic Pt-based anode catalysts for direct ethanol fuel cells. Journal of Power Sources, 131(1), 217-223.

Zuo, Y., Sheng, W., Tao, W., and Li, Z. (2022). Direct methanol fuel cells system–A review of dual-role electrocatalysts for oxygen reduction and methanol oxidation. Journal of Materials Science & Technology, 114, 29-41.